Biomed Eng Lett (2016) 6:181-195
DOI 10.1007/s13534-016-0222-6

REVIEW ARTICLE

Mechanical Characterization of Biological Tissues: Experimental Methods Based on Mathematical Modeling

Deok-Kee Choi

Received: 17 March 2016 / Revised: 3 June 2016 / Accepted: 8 June 2016

Abstract
Purpose To illustrate a systematic procedure for mechanical characterization or mechanical behavior of biological tissues with a semi-empirical method based on mathematical models.
Methods The method is composed of a series of procedures: construction of cell elements on the specimen, image processing, continuum mechanics, hyperelasticity and so on. An element used in the method, which is similar to finite element methods, is defined by placing markers on the specimen. The change of the locations of the element during a motion is monitored to calculate the displacement for stress estimation owing to external impacts or forces.
Results The validity of the method for mechanical characterization or mechanical behavior of biological tissues is shown through material test simulations with mathematical models, resulting in good agreement overall.
Conclusions A general review of mathematical modeling of biological tissues is served and a semi-empirical method, which makes good use of both finite element methods and mathematical models based on the phenomenological modeling technique, is introduced to assess the stress-strain responses of biological tissues subjected mechanical loadings.

Keywords Biological tissue, Hyperelasticity, Mechanical characterization, Soft tissue, Virtual surgery, Brain injury, Mathematical modeling.

INTRODUCTION

Studies on numerical simulations of biological tissues under physiological environment are growing popular for a long time owing to ever increasing demands from academia as well as industry. A fundamental procedure for establishing a mathematical model is to conduct a comparison of data generated from experiments and mathematical models. Once the model is validated with experiment data, it is ready for carrying out various numerical simulations. With the aid of the recent development in theoretical and experimental research on the field, more accurate material models to fit a broad scope of mechanical conditions have been developed. Despite the recent attempts in establishing a systematic modeling framework for biological tissues, it would take another decade or so to attain even a primitive goal close to the realness. Since experiments of biological tissues can be severely limited under various constraints, employment of numerical analysis is inevitable for studying a wide range of mechanical behavior subjected different mechanical conditions.

An extended review of recent mathematical modeling of biological tissues can be found in the literature [1, 2]. In order to get numerical simulations run correctly and efficiently, firstly a material model and experiment data must be given as primary input. A material model thus contains the parameters to be identified through many material tests such as tension, compression, biaxial and shear tests and so on. Once forece versus deformation relation is settled down on a form of a constitutive equation, it needs to be verified through numerical simulations conducted by means of numerical methods such as finite element methods. The range in which mathematical modeling is applied may be as large as the number of current biological materials. Furthermore, interesting subjects are of electrostatics, aortic aneurysms, anisotropic vascular membranes and anisotropic hyperelasticity with logarithmic strain, indentation and tensile measurement of the elastic modulus for soft tissues, compression material tests and development of the measurement of the ex vivo tissue samples.

Deok-Kee Choi (✉)
Department of Mechanical Engineering at Dankook University, Yongin 16890, Korea
Tel : +82-31-8005-3505 / Fax : +82-31-8021-7215
E-mail : dkchoi@dankook.ac.kr

There exist interesting studies on the nonlinear viscoelastic behavior of brain tissues and structures, human annulus fibrosis, vessel walls, porcine coronary artery tissue, collagenous soft tissues, skeletal muscle tissue, anisotropic hyperelastic modeling of soft tissues, Mullins softened filled rubbers, shearing of soft tissues and virtual reality machine being capable of realistic haptic response to medical doctors when touched. Furthermore, it should be mentioned that other issues have attracted attention recently: the recent maturation of modern techniques such as electromechanical modeling for human heart function simulation and identification of material properties of the ovine mitral valve in vivo via inverse finite element analysis, with installed radiopaque markers on the soft tissues to measure the shift during the cardiac cycles.

This article is organized as follows: Firstly, a discussion of rather a worldwide critique of the existing mathematical modeling of biological tissues is addressed as categorized as the accompanying sub-topics: measurement, rubber-like materials, brain tissues, blood vessels, virtual surgery machine and other biological tissues. Secondly, a procedure to set up mathematical models is laid out in detail. Lastly, an application of a semi-empirical method based on mathematical models to capture the behavior of biological tissues under mechanical loadings is clearly narrated with numerical examples.

MATHEMATICAL MODELING

It is obvious that the treatment of a whole range of mathematical modeling of biological tissues with various mechanical loadings is simply not possible; thereby only some of interesting works related to the modeling to be brought out in the present study will be referred. Mathematical modeling of biological tissues is a rather formidable task in every aspect, because it demands researchers be exposed to a huge amount of knowledge of continuum mechanics, mathematical analysis, and experiment data of chemical, biological and electrical features. Narrowing down the scope which will be apportioned in this article, hereafter only topics related with mechanical properties are brought up in particular. Once an appropriate mathematical model is constructed, yet impossible to incorporate exactly various external or internal mechanical conditions into experiments, an immediate benefit of which may be being able to numerically simulate mechanical behavior of soft tissues without conducting rather expensive experiments.

Fundamental material tests such as uniaxial tension, compression, biaxial tension and shear tests result in mechanical properties of soft-tissues, which can be best exemplified by the relationship between load versus stretch. A material model based on mechanical behavior of soft tissues, normally refers to a constitutive model, which presents the strain-strain responses to various mechanical loading conditions. Once experiment data are obtained, a curve-fitting to identify material parameters by minimizing the error between experiment data and a mathematical model is conducted. With the material parameters obtained from curve-fitting process plugged into a material model, the procedure for obtaining a mathematical model is complete and ready to be used in various numerical simulations.

There are two types of methods to construct mathematical models: One is about micro-structures of soft tissues; the other is about phenomenological method. The former is mostly theoretically oriented approach that requires accurate pieces of information on micro-structures of materials. Since a soft tissue consists of many different parts with different mechanical, electrical and chemical properties such as cells, fibers, and biological factors, mathematical models are extremely hard to be determined as a result. On the contrary, there exist somewhat simpler models, which may simplify complex structures of soft tissues, for example, a structure with only one or two differently aligned fibers in directions. Nevertheless, without fully understanding interactions among other elements, but the usage of more characters in mathematical models might not give good results to fit real world simulations. A core idea of the phenomenological modeling technique is as follows: a material model is rather directly related to experiment data that no a priori knowledge of micro-structure is necessary. Since a realm of micro-structure incorporated method is huge to deal with in a single article that in the present study only discussion on phenomenological method is directed. The phenomenological method, which mainly depends on curve-fitting methods with experiment data to identify the material parameters, is preferred among researches because of its simplicity compared to the theoretical method mentioned above. Thereby, only phenomenological modeling is discussed in the following section.

Rubber-like materials

Rubber-like materials are materials that consist of chain-like molecules closely connected to each other via cross connections. Soft biological tissues are in similar with rubber-like materials in terms of mechanical behavior; it is thus important to mention here mechanical characterization of rubber-like materials. As a result, many mathematical models based on rubber-like materials for various parts of human or animal body have been developed to date: brain tissues, arterial wall mechanics using chain extensibility constitutive models, heart and heart valve models, orthotropic active strain models, seat-cushion material models for passenger comfort and so on. A large collection of mathematical models of the materials has been established through frameworks of

hyperelasticity, which make use of energy density functions of hyperelastic materials to come up with the mechanical behavior of materials [3, 4]. Furthermore, an extensive study of the strain energy functions of different kinds of materials was performed [5]. Indeed, a lot of mathematical models of the materials have been announced from with least to most complexity. In fact, a simple elastic model cannot follow the mechanical behavior of rubber-like materials because of nonlinearity in both geometric nonlinearity and nonlinear constitutive equations at most cases. It is, thus, nonlinear models that fit to such nonlinearity should be employed. Several different approaches to obtain numerical data from material models have been proposed: a multi-scale model with micro-structures of rubber-like materials [6], a survey of different material models of rubber-like models [7], a model with compressibility and chain extensibility [8], slightly compressible materials [9]. Moreover, cases with complicated loadings such as monotonic or cyclic loadings, also have been proposed: a study on parameter identification of rubber-like materials under monotonic loadings [10]. Furthermore, under cyclic loadings consisting of simple tension and compression, rubber-like materials show nonlinear behavior that a linearity of stress-stretch relation does not fit in depicting the mechanical behavior of such materials. It is thus more elaborated constitutive models need to be used, in particular, the Mullins effect must be brought into account for embracing complex nonlinear mechanical behavior of rubber-like materials [11, 12].

Recent numerical methods available for material modeling incorporating experiment data as well as the mechanical behavior of materials are based solely on finite element methods because of their versatility and efficiency. Nevertheless, it is well known that numerical analyses of nonlinear mechanics problems are extremely difficult to deal with owing to nonlinearity; thus, various numerical schemes, material models and algorithms have been offered yet, just some of them are as follows: A study on finite element implementation of rubber-like materials was proposed [13], in which displacements, pressure and dilatations are treated as independent variables. In addition, a displacement-pressure algorithm has been applied to establish an elasto-plastic material model for rubber-like materials [14]. In order to deal with the incompressibility of a material with nonlinearity, the multiplicative technique onto the deformation gradient was suggested [15] and a three-field mixed formulation of a transversely isotropic model [16]. Moreover, a new algorithm, which can be applied to reduce the complexity of the finite element formulation owing to incompressibility of a material, was proposed, replacing a conventional framework of decoupling of deformation gradient with the proposed one [17]. It is also of interest to see an application of the inverse method with the known deformed configuration of incompressible material in order to design an object [18, 19]. In short, studies on mathematical models of rubber-like materials are still found attractive as an interesting research subject.

Brain tissues

It is reported that about four thousand people get a traumatic brain injury (TBI) each day in the United States [20]. Some excellent reviews on brain injury can be found in the literature [21, 22]. Moreover, it is interesting to see a study on mechanisms and mechanics of brain injury [23-25]. In addition, diffuse axonal injury (DAI) is one of the most common traumatic brain injuries, which injury occurs in moderate and mild brain injury in a specific area, occurring over even a wide area [26]. Also, numerical simulations with finite element methods on DAI was carried out [27]. Furthermore, there exist an important study, which is mainly focused on injuries in infants and young children [28, 29]. Identification of material parameters to construct mathematical models for axonal injury, which refers to the brain and spinal cord injuries, is extended out through the inverse methods, by which minimizing the error between the force-stretch curve from the calculation and the experiments [30]. It is therefore that brain tissue modeling must be closely linked with brain injury simulations or mechanisms. Since brain injury is primarily caused by a force, that is, tensile, compressive and/or shearing stresses, it is important to recognize how much stresses exerted on brain tissues when an impact are loaded. For instance, during an impact, the head is subjected to an external load and the payload is transported to the brain tissue in several ways. If the applied mechanical force on the brain tissue exceeds a certain level, brain injury would be occurred. Therefore, profound understanding of the event is strongly required to improve medical and mechanical measures and diagnosis of brain injury. Indeed, in order to calculate stresses, material models for brain tissues, which can convey constitutive relations as closely with experiment data as possible, are strongly required. However, a brain tissue is a quite delicate subject to study in many ways, in particular, from mechanical points of perspective. Besides its non-accessibility in vivo, having low mechanical stiffness makes it more difficult to install any stiffer sensors in order to detect motions or other physical entities during complex motions owing to an impact or an external force. Conventional experimental methods are about seeking displacements and stresses with data from various sensors installed on a specimen or an object: measurement devices are strain gauges, accelerometers, load cells, potentiometers and so on, which are all physically associated with the specimens. For instance, a set of strain gauges is used to account for the change in dimension of a specimen. Once measured data are collected from experiments, all is undergone with procedures that

result in a displacements or loads. Thus, displacements are utilized to calculate stress fields with the help of material constitutive equations. Nevertheless, a strain gauge is not practicable to measure the deformation of brain tissues. To simply put, the material is too soft to install the stiffer device on it. It is thus most experiments are performed with specimens in vitro. As a result, some studies on a comparison of experiments of in vivo versus in vitro or live versus dead tissues were reported [31-33]. A measurement of mechanical anisotropy of white matter, which is a part of a brain tissue, was carried out [34] as well as numerical simulation [30].

Since TBI is a most important and interesting topic, most researches on brain tissue modelings are also solely focused on seeking the mechanism of TBI occurring in the real world. In fact, the mechanical behavior of brain tissues can be changed significantly depending on types of external impacts or loads; thereby, it is necessary to investigate as many cases as possible. A broad review on the subject can be found in the literature [35]. It is obvious that researches on the subject may be divided into different categories according to type of impacts, models or external loading conditions. For example, a high rate tension device (HRTD) is developed to obtain dynamic properties of brain tissues, by which device experiment data are used to set up mathematical models for the dynamic properties of brain tissue based on hyperelastic models of Ogden, Fung and Gent [36]. Likewise, the effects of dynamic impacts were studied [37-39]. Likewise, written reports on the effect of rotational impact causing TBI have been proposed [40-44] and axisymmetric impact [45], torsional motions [46], compression [38] and tensions [47]. Mechanical impairment of brain tissue can be split into two classes depending on the mechanism of it: the volumetric and shear types. Finite element simulation based on an elastoplastic and a viscoelastic model of the brain injury owing to frontal and oblique head impacts is conducted [48]. In addition, a viscoelastic model is developed to simulate the dynamic behavior of porcine brain tissues. The material parameters are identified by fitting the model to the axial and volumetric test data. The robustness of the model are assured by comparing model predictions with the tissue response in compression at high strain rate and with data in uniaxial tension. This may thereby provide a mathematical model to be used with simulations of impact, leading to TBI [49] and numerical simulations were executed using viscoelastic models [50]. Also, numerical simulations with the framework of finite elasticity, by modeling a soft tissue as a homogeneous, isotropic, incompressible, hyperelastic material are conducted and compared with experiment data [51]. In order to set up a material model, one needs to have the parameters of a model fit to experiment data, which is called parameter identification [52]. Moreover, it is interesting to see the discussion of whether how much brain tissue can be regarded as incompressible in vivo [53]. More advanced subjects on TBI such as the coupling of fluid and brain tissues are found in the literature [54]. Even considering intensive researches to date, which have been performed successfully in both theoretical and experimental fields, it should be noted that the studies on brain tissues are far from mature; thus, further study is strongly required in the future.

Blood vessels

Each year 15,000 deaths owing to abdominal aortic aneurysm (AAA) in the United States are reported [55]. Aneurysm is a disease that stems from a local bulge of a blood vessel, for example, the aorta. A bulge swells with a constant pressure of moving blood over time. Once the size of the bulge reaches a critical value, it may collapse, putting a life in a severe danger. It is thus important to study mechanisms of aneurysm occurring in the aorta wall and mathematical models of blood vessels, in particular, to be used for calculation of the wall stress exerted by blood flow. Therefore, mathematical modeling of arterial walls and blood vessels has drawn much attention from the biomechanical field for years because the disease related to mechanical or physiological deterioration of blood vessels may cause severe health problems such as aneurysms. Hence, it is a principal goal of research to figure out an accurate wall stress distribution of blood vessels in vivo. The research sets out by applying mathematical models to be applied in mathematical analysis, which adjust the mechanical behavior of blood vessels. A pioneering attempt of mathematical modeling of arteries may start out with an introduction to pseudo-elasticity, which bears on the stress-strain relationship and the strain energy function based on hyperelasticity [56]. Primarily, mathematical models of the blood vessels are similar to rubber-like materials that many models are derived from rubber-like material models such as a model with chain extensibility.

As for various mechanical characteristics of blood vessel, the strain-hardening, which refers to a phenomenon of revealing nonlinear stress-strain behavior, with higher extensibility in the lower stretch range and progressively lower extensibility with increasing stretch when uniaxial tests on vascular walls are studied. In order to capture this, power-law models and limiting chain extensibility models are viewed in a vertical string of arterial tissue and an internally pressurized cylindrical tube, which are compared with the experiment data [57, 58] as well as experimental approach was conducted [59]. Blood vessels have been mostly considered as an incompressible matter for the sake of simplicity in both theoretically and experimentally; however, owing to the complexity of deformation, it is quite interesting to verify the compressible property observed in many experiments [60-62]. A blood vessel consists of multiple layers with different mechanical properties and micro-structures that it is quite

challenging to define comparable material models, which thus should not be considered as a simple homogeneous isotropic material. A more elaborated model is composed of matrices and randomly aligned fibers, which produces anisotropy and the nonlinear anisotropic elastic behavior of healthy porcine coronary arteries is studied [63]. Besides the properties and structures, it is known that blood vessels are subjected to residual stresses in vivo, which inclines to get the modeling more complicated. Since it is impossible to bring into account every boundary condition exerting tissues in vivo, development of the mathematical models has been confined to employment by kind of simpler ones. Thus much study has focused on the subject of hyperelastic elastic model with fibers through continuum mechanics framework. For example, hyperelastic modeling of arterial layers with distributed collagen fiber orientations is conducted [64]. More researches on the wall stress have been performed to date [65-70] and it is obvious the wall stress may change depending on the model used in aneurysm computer simulation, for example, a comparison of modeling technique was reported [71] and for a three-dimensional model [72]. For mathematical models to be used in various mechanical loading conditions, other than uniaxial test such as biaxial test or shear test should be carried out. Compared to uniaxial test, it is more expensive to conduct biaxial test or shear test owing to the increasing complexity of experiment device. With biaxial testing device, an equal force is applied to each side of a thin tissue. It is of interest to study the mechanical behavior of arterial walls or blood vessels when higher physiological blood pressure applies in a cyclic manner to them and physiological pulses may be simplified as cyclic pressure or tension-compression loadings. Hence, blood vessels may become damaged due to excessive physiological loadings over time. Also, a damage model is built up with a continuum damage assumption [73]. In addition, a modeling failure criterion was suggested in the form of an energy limiter [74].

Other than modeling of blood vessels, it is recognized that the interaction between arterial walls and blood flow can play an important role to expand the size of an aneurysm; hence such an advanced topic with a fluid-solid coupling has been actively studied [75-78]. It is interesting to acknowledge that the comportment of the constraint of the tissues nearby should be hired into consideration when in vitro and in vivo measurements of the mechanical attributes of vascular vessels are conducted. A fact that surrounding tissues also can ingest a substantial quantity of the intravascular pressure that reduce a good sum of the wall stress was described [79]. Furthermore, application of medical images is getting popular to study aneurysms: the stability of aneurysms was studied with the help of abdominal CT images [80] and the interaction between blood flow and vessel wall was performed based on medical images [81].

Unlike most researches about a mechanical side of aneurysm mechanism, interestingly, the effect of calcifications on the wall stress was studied [82]. In addtion, some other topics on aneurysms are also announced, for example, the effect of age and pressure on the wall stress [83], the strain energy density function for arteries obtained fro topographical sites [84], local mechanical properties of aneurysms [85], and automatic generation of surface topologies for aneurysm models [86].

The motion of cardiac tissue is energized by electromechanical momentum; thereby, it is important to take into account field variables of electro-physiology and electromechanics, which are coupled in the governing equations. The coupled reaction-diffusion equations for the electrical problem and the momentum equations for the mechanical part transform into weak forms to be implemented in finite element methods. A stable algorithm and mixed finite element formulation are studied to solve the multi-physics problem [87]. Mathematical modeling of cardiac tissue is also of interest through acknowledgement of two major different characteristics: passive and dynamic properties. In order to imitate the motion of cardiac tissue, a material model that is capable of capturing both properties should be prepared. Both of the schemas are considered with passive and active deformation to yield behavior simulations of cardiac tissue [88].

Other biological tissues

A study on the annulus fibrosis, which is the wrapping that takes up the outside portion of the intervertebral disc protecting the nucleus pulposus located in the center of the disc, is indefensible for human to live a healthy life because degeneration and ageing can lead to joint pain. By employing hyperelasticity and continuum mechanics, a strain energy that comes up with different constituents such as matrix, fibers, and other elements and the interactions among them, is developed to be used for numerical simulations [89]. A study of the passive length-tension properties and the active response of skeletal muscle tissue is conducted to develop mathematical models [90]. Mathematical models of skeletal models are important to improve seating comfort, which is directly related to the seat and the seated-human/seat interactions. The interactions among bones, skins, and seats should be considered as a core subject to provide passengers with better quality of seating comfort [91]. Stress calculation in osteoarthritis of the knee was conducted [92] and a strain analysis of soft biological membranes is also reported [93].

Measurement techniques

If one can come up with an accurate stress distribution of blood vessels in vivo, more reliable material models could be developed. However, stress estimation of the tissues in vivo is simply not possible owing to many difficulties including

ethical issues. Thus, in order to circumvent such unsolved problems, a noninvasive approach such as a method with in vivo image can be established. Thereby the image is considered as a deformed tissue in vivo. Once the initial shapes of the tissues are known with an inverse analysis, a patient-specic abdominal aortic aneurysm model can be set up [94, 95]. In order to obtain the material properties of mitral valve (MV) leaflets in vivo, miniature radiopaque markers are sewn to the MV annulus and the coordinates of biplane video fluoroscopic marker images are also obtained during three complete cardiac cycles. With the obtained data to be used to identify the material parameters of a mitral valve model, it is expected that one may be able to simulate the dynamic motion of the valve [96]. As studies with conventional material tests such as a uniaxial tensile test and compression test to find the material parameters to set up mathematical models grows, recently new measurement techniques have emerged such as imaging technology with high-tech device. For example, elastography is proposed to image tissue elasticity based on imaging methods collectively called elastography. While progress in developing these systems has been rapid, the basic understanding of tissue properties to interpret elastography images is mostly lacking. The measurement technique consists of indenting an unconfined small block of tissue while measuring the resulting force. The elastic modulus of the tissue is constructed from the measured displacements using an inverse method with the help of elstography technique [97].

There is another measurement technique for tissue elasticity based on magnetic resonance elastography in which a tissue specimen encased in a gelatineagarose block undergoes cyclical compression with resulting displacements measured using a phase contrast MRI technique: Young's modulus measurements of soft tissues [98-100], for mechanial properties of breast tissues [101] and the use of three-dimensional finite element modeling using MRI data [102].

Virtual reality surgery machine

One of premium results of mathematical modeling of biological tissues may be something that is linked up to computer-integrated or robot-aided surgery machine, which could be utilized as an automatic surgical device in case of emergency where no doctor is available for surgical operation. In order to have an automatic surgical tool or machine to do such life-saving procedure for patients, the realistic material response must be provided by the mechanical properties of the tissues activated accordingly. In the close future, it may be anticipated that medical students or physicians may practice realistic surgical operation with the patient specific virtual machine. If one can come up with accurate mathematical models of important soft tissues like brain, kidney, and liver and so on, inexpensive surgical practice with the virtual machine may become huge benefit to both patients and doctors. In order to set up virtual surgical machine, establishing mathematical models that can simulate the behavior of tissues and the interactions between surgical instruments and tissues is a primary task. Instead of simple linear elastic models, the nonlinear model is enforced to the simulation to have a more realistic mechanical response [103]. An algorithm for the mechanical behavior of soft tissues is developed to be applied to real-time surgical simulation, which is based on finite element methods. In order to avoid numerical instability, the explicit time integration is employed [104].

Another interesting application of computer based medical machine is about fittings of a prosthetic socket because a misfit can cause pressure ulcers or a deep tissue injury (DTI: necrosis of the muscle flap under intact skin) in the residual limb. A real-time patient-specific finite element method is set up to provide better fittings of a prosthetic socket, which is an extremely important step in the process of rehabilitation of a trans-tibial amputation (TTA) patient [105]. A mathematical model with nonlinear response of living tissues, the nite element simulation of palpation a human cornea is carried out [106]. The heart is a most important, yet complex organ that the volume of research on the establishment of mathematical models is large in quantity. Under cardiac cycles, the heart system consisting of four different chambers makes it extremely difficult to set up an accurate model to be used for numerical heart simulations. Furthermore electro-mechanical behavior of the heart makes the modeling even more complicated. Computer simulation of the heart is conducted with respect to electro-mechanical governing equations [107]. It is of interest that a brain tissue model was proposed upon surgical procedure simulations [108].

PHENOMENOLOGICAL MODELING

In this section, a brief introduction to the phenomenological modeling is addressed. The phenomenological modeling is a modeling technique that makes the use of both a mathematical model and experiment data. A key notion of this modeling is about not concerning the micro-structure of the tissue, but considering the use of the combination of a material model and the corresponding experiment data. A collaboration of a mathematical model and corresponding experiment data is an essential procedure for the identification of mechanical parameters. Interestingly, most mathematical models available to date are based on hyperelasticity, which is a solid theoretical ground for various soft tissues because of its simplicity in the derivation of stress versus strain relation. Taking a derivative of a strain energy function with respect to deformation or strain to obtain a stress-strain relation is a rather simple procedure compared to the use of other material models such

as hypoelastcity-based models. Thus, stress can be expressed as a function of strain without considering the deformation history, which gives researchers much freedom in testing various mathematical models to meet different realistic conditions. There are a few material models based on hyperelasticity such as neo-Hookean, Mooney-Rivlin, Ogden and so along. Prilimarily, biological soft tissues are mostly incompressible, which means the volume preserves during large deformation. The significant ingredients of soft tissues are nonlinear elastic, isotropic, incompressible and independent of strain rate. In this section a procedure of defining a mathematical model for biological tissues based within the phenomenological way is addressed [109].

The neo-Hookean model [1, 2], which is one of the simplest models with a single parameter μ to be determined, for which the hyperelastic energy function $\psi(\Lambda)$ is given by:

$$\psi(\Lambda) = \frac{\mu}{2}(\Lambda_1^2 + \Lambda_2^2 + \Lambda_3^2 - 3) \tag{1}$$

where Λ_1, Λ_2 and Λ_3 are the stretches in the three principal directions, respectively. For example, as for a uniaxial tension with incompressibility, refer to Table 1 for the stretch data. In fact, the nominal stress T^{math} is obtained by

$$T^{\text{math}} = \frac{\partial \psi(\Lambda)}{\partial \Lambda} = \mu\left(\Lambda - \frac{1}{\Lambda^2}\right) \tag{2}$$

The strain-strain response for a uniaxial tensile test, thus can be obtained with Eq. (2) along with the stretches corresponding to the experiments. Similarly, the stress-stretch relations from the other tests such as biaxial and shear tests can be also calculated with the data listed in Table 1 without any difficulties. The plot of the stress-stretch response of three different tests, uniaxial, biaxial and shear tests, are also shown in Fig. 1. It is interesting to see the results from the uniaxial test and biaxial test show a significant discrepancy between two different tests, whereas the difference between the uniaxial test and pure shear test can be so small that two results appear identical. Indeed, the large discrepancy prompts that different tests other than uniaxial tests should be conducted to capture complex mechanical behavior of biological tissues; thereby a mathematical model should also be installed in order to be integrated with a extensive range of movements and loading conditions. Differently, it should be mentioned that a simple mathematical model based only on uniaxial test may not correctly interpret the mechanical behavior of biological tissues in many complex cases of mechanical loadings.

Typical material tests consist of simple tension, compression, biaxial, simple shear, pure shear, and volumetric compression. It should be mentioned that the tests need to be conducted in principal stretch mode so that the mathematical formulation of materials may be made without conducting complex calculation owing to the transformation of coordinates. Once multiple tests are posted out, obtained data are set out into a curve fitting routine in order to identify material parameters through the following form:

$$\min_{\mu} \sum_{i=1}^{N} [T_i^{\text{exp}} - T_i^{\text{math}}(\mu)]^2 \tag{3}$$

where N is the number of data. That is, minimizing the stress error or difference between those of experiment T^{exp} and mathematical model T^{math} in Eq. (3) with respect to unknown parameters completes a material identification procedure. For example, it is required of a material parameter μ of the neo-Hookean model. In fact, there exist various curve-fitting algorithms among which the least-square fitting is most popular. Hence, it is noted that the definition of the error need not be the same as above. Other forms of errors such as relative error can be also defined to meet any specific interest. For example, if three different experiment data from uniaxial, biaxial, shear experiments are available, one may

Table 1. The corresponding stress and stretch for three different tests, where T^{exp} being the nominal stress defined as F/A_0, that is, the ratio of the force applied F to the initial cross-sectional area A_0 of a specimen. The stretch ratio Λ is defined by l/l_0, where l is the current length and l_0 the initial length of a specimen. The change in length of a specimen and the applied force can be easily collected through experiment device such as a universal testing machine, which are converted into nominal stress versus stretch ratio diagram.

Experiment	Stress	Stretch
Uniaxial tension	T^{exp}	$\Lambda_1 = \Lambda$, $\Lambda_2 = \Lambda_3 = 1/\sqrt{\Lambda}$
Biaxial tension	T^{exp}	$\Lambda_1 = \Lambda_2 = \Lambda$, $\Lambda_3 = 1/\Lambda^2$
Pure shear	T^{exp}	$\Lambda_1 = \Lambda$, $\Lambda_2 = 1$, $\Lambda_3 = 1/\Lambda$

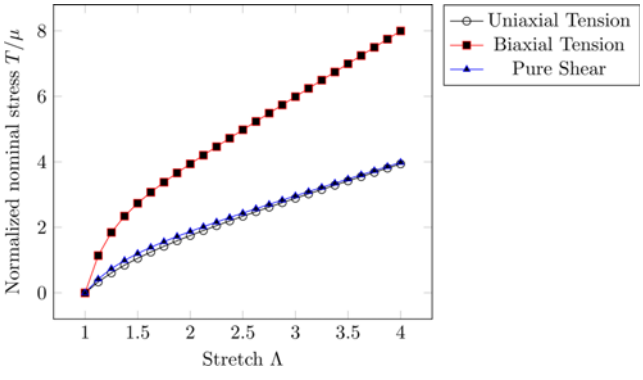

Fig. 1. The plot of the normalized nominal stress (T/μ) versus stretch Λ generated with the neo-Hookean material model in Eq. (2) subjected to a uniaxial, biaxial and pure shear tests, respectively. The material parameter of a mathematical model is to be determined via curve-fitting technique with accordance with experiment data.

define the least-square type of error as follows:

$$\min_{\mu} \left\{ \sum_{i=1}^{N} (T_i^{\exp} - T_i^{\text{math}})^2_{\text{uniaxial}} + \sum_{j=1}^{M} (T_j^{\exp} - T_j^{\text{math}})^2_{\text{biaxial}} + \sum_{k=1}^{S} (T_k^{\exp} - T_k^{\text{math}})^2_{\text{shear}} \right\} \quad (4)$$

where N, M and S are the number of respective experiment data. Similarly, by minimizing the error in Eq. (4) with curve-fitting algorithms, the material parameters can be obtained, which completes the whole procedure for a mathematical model.

SEMI-EMPIRICAL METHOD

It may be not always guaranteed that the results from numerical simulations could represent the mechanical behavior correctly, in particular, under complex loadings or motions. To answer this difficult question, all necessary conditions arising during experiments such as mechanical boundary conditions of biological tissue specimens must be recognized and converted as inputs into the computer program for numerical simulations; however, it is just not possible to reckon all information of these boundary conditions.

In this segment, a semi-empirical method, which is called the cell element method, is presented to capture the mechanical behavior of a biological tissue under complex mechanical motions or loadings. A key concept of the method is about only having displacement data to be employed for the stress calculation; thus, the estimation of stress in a deformed portion of a tissue can be obtained by taking snapshots of the apparent movement of cell elements owing to forces or motions. This method consists of a series of experiments and numerical procedures: preparation of specimens, construction of cell elements, image processing and deformation calculation and so on.

As an instance of application of the method, it necessitates to be made in such a way that three markers are set along a specimen in order to build a triangular element shown in Fig. 2. That is, the cell element is a term to denote a physical element constructed by markers placed on a specimen. Once the element is constructed, snapshots are taken with the high-speed camera shown in Fig. 3 during a motion owing to external forces, which then to be processed by an image-processing program to generate the coordinates of the element in the current configuration. The deformation of the element thus can be held with the mapping among the configurations: the parent, the initial, and the current

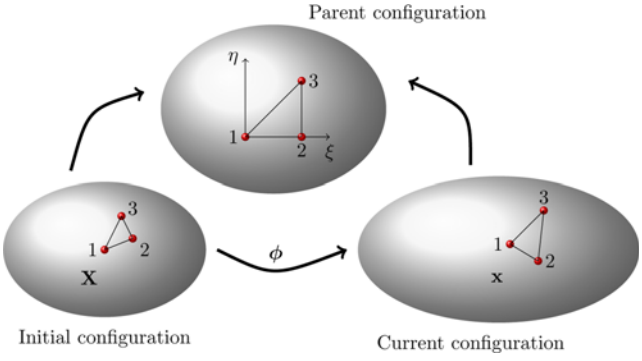

Fig. 2. Schematic of the coordinate transformation: Three red markers representing the nodes of a triangular element are set on the surface of a soft tissue. A change of the coordinates between the initial configurations and the current configuration owing to external forces is observed upon a change of three markers' locations. The mapping function $\mathbf{x} = \phi(\mathbf{X})$ maps the initial material point $\mathbf{X}$ into the current coordinates $\mathbf{x}$. By adopting isoparametric elements, the elements in the initial configuration and the current configuration are readily transformed into that in the parent configuration to be used for the cell element method.

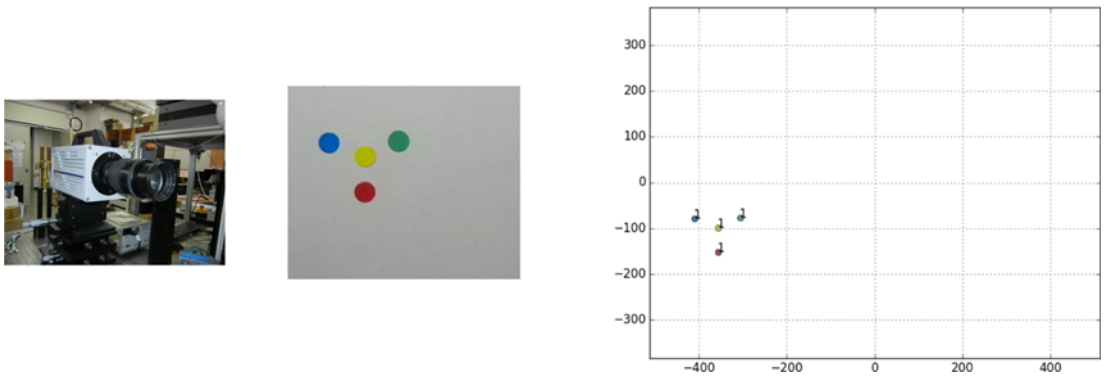

Fig. 3. *Left*: The high-speed camera capable of capturing up to a thousand frames per second, which can track down the motion of the markers on the specimen. *Center*: The photo taken with the high-speed camera. *Right*: The result of executing the image-processing program with the photo taken. The image-processing program, written in *Python* script language, successfully recognizes the markers' coordinates on a specimen.

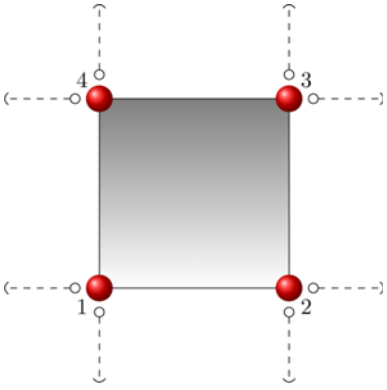

Fig. 4. A quadrilateral cell element with four nodes of which coordinates are (0.0), (1,0), (1,1) and (0,1) for node 1, 2, 3 and 4, respectively.

configurations as shown in Fig. 2. In the figure, only three markers are used to construct a triangular finite element; however, the number of markers can be easily added depending on what type of an element has to be employed. For example, two markers can be placed in an interval element and a quadrilateral element for four markers shown in Fig. 4, respectively.

The coordinates of the markers or nodes in the initial configuration are denoted as **X**, which is addressed as the material points. The current coordinates are expressed as **x**. The displacement **u** denotes thus merely the difference between those two coordinates: $\mathbf{u} = \mathbf{x} - \mathbf{X}$. The calculated displacements are to be used as boundary conditions for a cell element. The calculation of the changes in the coordinates of the element between two different configurations is of a most importance. Employing kinematics, a motion of the element can be identified with the mapping function ϕ connecting two coordinates each other as shown in Fig. 2 and is expressed in the form: $\mathbf{x} = \phi(\mathbf{X})$, where ϕ is the mapping function interacting between two frames. Moved over the cell element concept, the markers are handled as the nodes of finite element methods. The cell element is thus constructed with the markers on the specimen. It is more useful for isoparametric element to be processed in the cell element method because types of cell element don't need to be confined to a triangular finite element with a right angle shown in Fig. 2. This means that there is much freedom to decide the locations of markers in the initial form. The initial and the current coordinates are expressed in terms of the nodal values and the shape functions. The shape function is defined in the parent configuration; that is, $N(\xi)$ where ξ is the parent coordinate. Hence the current coordinates are given as $\mathbf{x}(\xi) = \sum_{I=1}^{n} N_I(\xi)\mathbf{x}_I$, where n denotes the number of nodes in an ingredient. Likewise, the coordinates in the initial configuration are expressed in the form: $\mathbf{X}(\xi) = \sum_{I=1}^{n} N_I(\xi)\mathbf{X}_I$. Note that both the initial and current coordinates are expressed in terms of the shape function in the parent form. The coordinates of the markers are expressed as $\mathbf{X}_I$ for the initial configuration and $\mathbf{x}_I$ for the current configuration. Employing the concept of isoparametric elements widely used in finite element methods, the coordinates of the location of three marked points are given in terms of the shape functions and nodal values of the deformed element $\mathbf{x} = \sum_{\alpha=1}^{n} N_\alpha \mathbf{x}_\alpha$. The deformation gradient **F** plays an important role to depict the motion of a cell element, which is defined by

$$\mathbf{F} = \text{Grad } \mathbf{x} = \sum_{I=1}^{n} \mathbf{x}_I \text{ Grad } N_I \tag{5}$$

where Grad is the gradient with respect to **X** and

$$\text{Grad } N_I = \frac{\partial N_I}{\partial \xi}\frac{\partial \xi}{\partial \mathbf{X}} = \left(\frac{\partial \mathbf{X}}{\partial \xi}\right)^{-T}\frac{\partial N_I}{\partial \xi}, \ \frac{\partial \mathbf{X}}{\partial \xi} = \sum_{I=1}^{n} \mathbf{X}_I \frac{\partial N_I}{\partial \xi} \tag{6}$$

In the final stage, the last procedure of the cell element method for stress calculation is exemplified through the accompanying examples in the following segment.

Variational formulation

The mechanical behavior of such a material has been known by employing hyperelastic material models. With the help of the mathematical model, the stress can be simply obtained from an elastic energy function by conducting some mathematical manipulations. Once a hyperelastic material model is put on a test to fit experiment data in terms of a constitutive relation, numerical analysis are required among which finite element method stands out to calculate the mechanical behavior of the material under various complex boundary conditions. It is the variational formulation on which finite element method is mathematically based; thereby, a brief introduction to this formulation of nonlinear problems is given as follows [14, 110].

The potential energy Π of a material over the domain Ω and the boundary Γ subjected to boundary conditions is given by

$$\Pi(\mathbf{F}, \mathbf{u}) = \int_{\Omega} \Psi(\mathbf{F}) dV - \int_{\Gamma} \overline{\mathbf{T}} \cdot \mathbf{u} dA \tag{7}$$

where Ψ is the hyperelastic energy function and $\overline{\mathbf{T}}$ is traction at the boundary Γ. The stationary condition for the potential energy in Eq. (7), i.e. $\delta\Pi = 0$ is expressed as

$$\delta\Pi = D\Pi[\delta\mathbf{u}] = \int_{\Omega} \frac{\partial \Psi}{\partial \mathbf{F}} : \delta\mathbf{F} dV - \int_{\Gamma} \overline{\mathbf{T}} \cdot \delta\mathbf{u} dA \tag{8}$$

where $\delta\mathbf{F} = \text{Grad } \delta\mathbf{u}$ and D is the directive derivative. If the stationary condition is enforced by figuring out the equation $\delta\Pi = 0$ for the displacement, strains and stresses would be

derived accordingly. However, hyperelastic material models for a soft tissue are usually nonlinear with respect to the displacement. Therefore, Eq. (8) needs to be linearized with respect to the displacement.

For the sake of brevity, it is convenient to employ an abstract framework hereafter. According to the functional analysis theory, an approximate solution (finite-dimensional solution) to a problem must be sought in an appropriate solution space. The solution space V is defined as $V = \{\mathbf{u}|\mathbf{u} \in H^1(\Omega), \mathbf{u} = \bar{\mathbf{u}} \text{ on } \Gamma\}$, where $H^1(\Omega) = \{\mathbf{u} \in L^2(\Omega)|\ \text{grad}, \mathbf{u} \in L^2\}$, $L^2(\Omega) = \{v|\int_\Omega v^2 dx < \infty\}$ and $\bar{\mathbf{u}}$ is the displacement boundary condition on Γ. Converting the variational form in Eq. (8) into an abstract form to yield a problem of finding a function $\mathbf{u} \in V$ such that

$$a(\mathbf{u}, \delta\mathbf{u}) = l(\delta\mathbf{u}) \qquad \forall \delta\mathbf{u} \in V \tag{9}$$

where $a(\bullet, \bullet)$ is the bilinear form $a : V \times V \to \mathbb{R}$ and $l(\bullet)$ is the linear form $l : V \to \mathbb{R}$ and

$$a(\mathbf{u}, \delta\mathbf{u}) \equiv \int_\Omega \frac{\partial \Psi}{\partial \mathbf{F}} : \delta\mathbf{F} dV, \quad l(\delta\mathbf{u}) \equiv \int_\Gamma \overline{\mathbf{T}} \cdot \delta\mathbf{u} dA$$

Since the solution $\mathbf{u}$ to Eq. (9) is not exact but approximate that the residual $R(\mathbf{u})$ is inevitable to exist as follows:

$$R(\mathbf{u}) = a(\mathbf{u}, \delta\mathbf{u}) - l(\delta\mathbf{u}) \tag{10}$$

Since the residual equation Eq. (10) is nonlinear that it needs to be linearized in the direction of $\Delta\mathbf{u}$:

$$DR(\mathbf{u})[\Delta\mathbf{u}] = \hat{a}(\mathbf{u}; \Delta\mathbf{u}, \delta\mathbf{u})$$

where

$$\hat{a}(\mathbf{u}; \Delta\mathbf{u}, \delta\mathbf{u}) \equiv Da(\mathbf{u}, \delta\mathbf{u})[\Delta\mathbf{u}], \quad Dl(\delta\mathbf{u})[\Delta\mathbf{u}] = 0$$

also an explicit form:

$$\hat{a}(\mathbf{u}; \Delta\mathbf{u}, \delta\mathbf{u}) = \int_\Omega \delta\mathbf{F} : \frac{\partial^2 \Psi}{\partial \mathbf{F} \partial \mathbf{F}} : \Delta\mathbf{F} dV + \int_\Omega \frac{\partial \Psi}{\partial \mathbf{F}} : \Delta\delta\mathbf{F} dV$$

Employing an iterative numerical scheme such as Newton-Raphson algorithm to solve the nonlinear equation in Eq. (10),

$$\hat{a}(\mathbf{u}^k; \Delta\mathbf{u}^k, \delta\mathbf{u}) = l(\delta\mathbf{u}) - a(\mathbf{u}^k, \delta\mathbf{u}) \tag{11}$$

where k is the iterative index and $\Delta\mathbf{u}^k = \mathbf{u}^{k+1} - \mathbf{u}^k$. Eventually, the iterative process for solving Eq. (11) continues until the designated error condition is met.

RESULTS AND DISCUSSION

In summary, it is noted that the cell element method makes use of a collaboration of experiment data as well as the finite element concept originated from finite element methods in order to obtain stress induced when a specimen is subjected to complex motions. This method thus consists of three distinctive steps: **Cell element → Image capture & processing → Stress calculation**. What follows is a brief explanation of the tests. In the first step, a construction of a cell element on a specimen is done by placing markers(nodes) on it. The movement of the nodes owing to external forces or impacts is also captured with a high speed camera. Based on the movement of the nodes, the displacements of these nodes are easily determined to be used for determining the deformation gradient. Ultimately, this gradient is used to obtain the stress in Eq. (13). This concludes the procedure typically performed in the cell element method.

In order to verify the validity of the cell element method, we have conducted three numerical examples simulating different material tests, which are biaxial tension tests, simple shear tests, and a complex motion test. Note that all the instances in the present work were done with fictitious data; yet, the method can be promptly applied to various experiments, keeping most part of the method unchanged. Throughout the examples, a soft tissue based on the compressible neo-Hookean model [1, 2] was used for which energy function is given by

$$\Psi = \frac{\mu}{2}(\text{tr } \mathbf{C} - 3) - \mu \ln J + \frac{\lambda}{2}(\ln J)^2 \tag{12}$$

where the right Cauchy-Green tensors $\mathbf{C} = \mathbf{F}^T \mathbf{F}$, the Jacobian $J = \det\mathbf{F}$ and the material parameters $\mu = E/(2(1 + \nu))$ and $\lambda = E\nu/((1 + \nu)(1 - 2\nu))$ with elastic modulus $E = 1{,}000$ Pa and Poisson's ratio $\nu = 0.4$. The Cauchy stress is typically defined in the form:

$$\boldsymbol{\sigma} = J^{-1} \frac{\partial \Psi}{\partial \mathbf{F}} \mathbf{F}^T \tag{13}$$

Once the deformation gradient is determined along with respective motions, the stress can be calculated with Eq. (13).

As the first example, two directions of the specimen as shown in Fig. 4 being perpendicular to each other are loaded with tensile forces, respectively. That is, biaxial tension tests were performed with a quadrilateral element of which coordinates of the nodes are given by (0,0), (1,0), (1,1) and (0,1), respectively. The results are given in four different cases: ($\lambda_1 = 0.05$, $\lambda_2 = 0.05$), ($\lambda_1 = 0.1$, $\lambda_2 = 0.1$), ($\lambda_1 = 0.05$, $\lambda_2 = 0.1$) and ($\lambda_1 = 0.1$, $\lambda_2 = 0.15$) for cases *A*, *B*, *C* and *D*, respectively. Moreover, the deformation gradient of the biaxial tension test is $\mathbf{F} = \lambda_1 \mathbf{e}_1 \otimes \mathbf{e}_1 + \lambda_2 \mathbf{e}_2 \otimes \mathbf{e}_2 + \mathbf{e}_3 \otimes \mathbf{e}_3$. In order to obtain the displacement, four marked points are used as nodes as shown in Fig. 4. Once the displacement is known through captured images, the stress can be readily calculated with Eq. (13). Numerical simulations for the comparison are also made with 983 finite elements for finite element methods

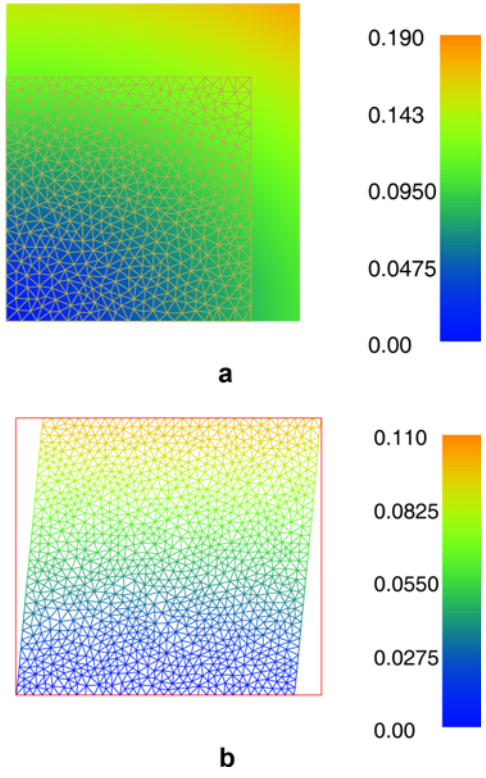

Fig. 5. The simulation results from two different material tests: (a) Finite element model with 983 finite elements for the biaxial simulations, (b) Finite element model with 2244 finite elements for the simple shear test simulations (γ = 0:1).

as shown in Fig. 5a. Finally, the comparison between the biaxial test simulations of the cell element method and finite element methods is shown in Fig. 6, this comparison of stresses obtained between two methods shows an excellent agreement over four different cases. It is thus concluded that the cell element method can be used for typical material tests such as biaxial tension test.

As the second example, simple shear tests are performed for $\gamma = 0.1 \sim 0.5$, where γ is the shear strain. Thereby, the deformation gradient for a simple shear test is $\mathbf{F} = \mathbf{e}_1 \otimes \mathbf{e}_1 + \gamma \mathbf{e}_1 \otimes \mathbf{e}_2 + \mathbf{e}_2 \otimes \mathbf{e}_2$. The finite element model is composed of 2,244 finite elements as shown in Fig. 5b. Upon observing the results shown in Fig. 7, as it is expected that the shearing stress is not quite going well at the comparison. There might be a few reasons of discrepancy, one possible reason among which may be the use of a constant strain element when shear strain $\gamma > 0.1$. In this situation, given severely distorted elements owing to a large shear deformation, even simply increasing the number of finite elements seems to be no help to thin out the errors. The calculated shearing stress with the cell element might be overestimated as the shear stress increases. Since only four nodes are employed for a cell element in this example, it may be hardly to get accurate results unless going with more elements. On the other hand,

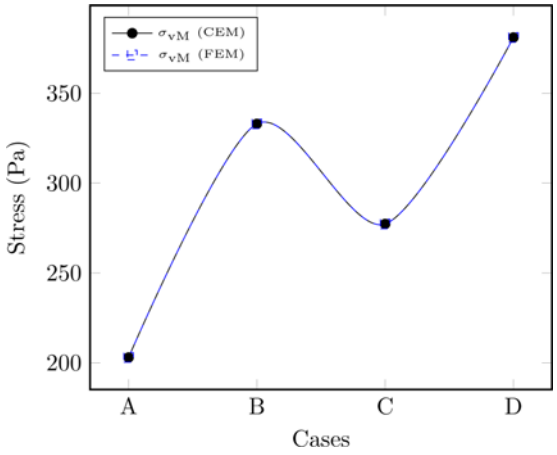

Fig. 6. Comparison of von Mises stress vs stretch relations for biaxial tension test simulations of the cell element method and finite element methods. The biaxial tension tests are done with a quadrilateral element for four different cases: ($\lambda_1 = 0.05$, $\lambda_2 = 0.05$), ($\lambda_1 = 0.1$, $\lambda_2 = 0.1$), ($\lambda_1 = 0.05$, $\lambda_2 = 0.1$) and ($\lambda_1 = 0.1$, $\lambda_2 = 0.15$) for cases *A*, *B*, *C* and *D*, respectively.

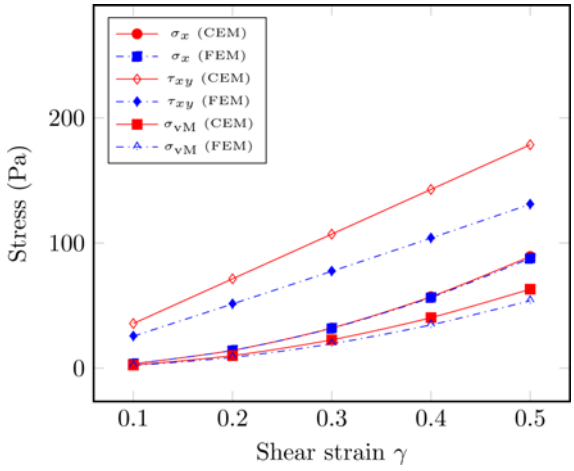

Fig. 7. Comparison of stress versus shear strain obtained the cell element method and finite element methods.

an advantage of the cell method is that it takes just over a small part of a specimen not the entire domain for calculation; therefore, relatively poor results are understandable by the use of a single element. A remedy for the error may be use of higher degree elements; even so, it is out of scope in the present work.

The last example is of complex motions owing to external forces or impacts. The simulation is performed with a triangular element in four different cases listed in Table 2. It is also noted that the coordinates of the element in *A* denote the initial configuration of the element and the others represent some other situations owing to different boundary conditions generated through external forces or impacts. The simulations were conducted in such a fashion that the motion

Table 2. Fictitious experiment data for the cell element method. The coordinates of the nodes of the triangular element in the initial coordinate in *A* and three different configurations in *B*, *C* and *D*.

Nodes	A	B	C	D
1	(0.0, 0.0)	(0.3, 0.1)	(0.6, 0.3)	(0.8, 0.5)
2	(1.0, 0.0)	(1.4, 0.3)	(1.4, 0.6)	(1.5, 0.9)
3	(1.0, 1.0)	(0.6, 1.1)	(0.3, 0.9)	(0.9, 1.3)

of the element begins at configuration *A*, and then it shifted to next configurations *B*, *C* and *D* in turn. As is seen in Fig. 8, the stresses were tracked down over the time sequences from *A* to *D*. The results confirm that the cell-element method can be used for obtaining kinematic motions as well as stress calculation of a specimen subjected to complex loadings. Furthermore, it can be deduced that the more complex motion applies, the more segments needed for the entire movement.

We have demonstrated that the cell element method can play an important role to grab up the motion of a soft tissue subjected to an external force or an impact. With a high-speed camera, instantaneous motions of the specimen in responding to external stimuli can be captured to be used to measure the deformation. An in-house image processing program written in *Python* script language successfully identifies the coordinates of the elements from the images taken with the camera as shown in Fig. 3. For example, three nodes are to construct a triangular element on the surface of a soft tissue and the camera takes pictures of the specimen during the motion. The pictures are shipped to be processed through an image-processing program to key out the coordinates of the nodes automatically. Thus, the obtained coordinates are to be employed as an input for the cell element program. Throughout the examples, the cell element method is carefully examined to see if it works in various situations correctly. In order to reduce the numerical error, as mentioned before, the size of a cell element needs to be smaller, which means the markers should be placed closer together when placed on a specimen. Since finite element methods are of an entire domain, if such a complicated motion applies as shown in Fig. 8, it is awkward to find appropriate boundary conditions. On the reverse, the cell element method requires information on the coordinates of a diminished part of the consistence, that is, only the displacement boundary conditions are needed. Thus, the method may find its best usefulness in those fields where local stress estimation is needed, such as brain damage estimation in car accidents.

CONCLUSION

The article starts out with a general review of mathematical modeling of biological tissues yet focused on the phenomenological modeling, which only considers overall mechanical behavior compatible with experiment data. In the phenomenological modeling framework, a mathematical model with material parameters can be established by minimizing the error between a hyperelastic material model and the corresponding experiment data with curve-fitting algorithms. Once a mathematical model is obtained, it can be implemented in finite element methods for diverse forms of numerical simulations. However, it is difficult for numerical simulations take into account every mechanical condition arising in real world situations. Furthermore, a soft tissue, such as a brain tissue will not allow any sensors made of

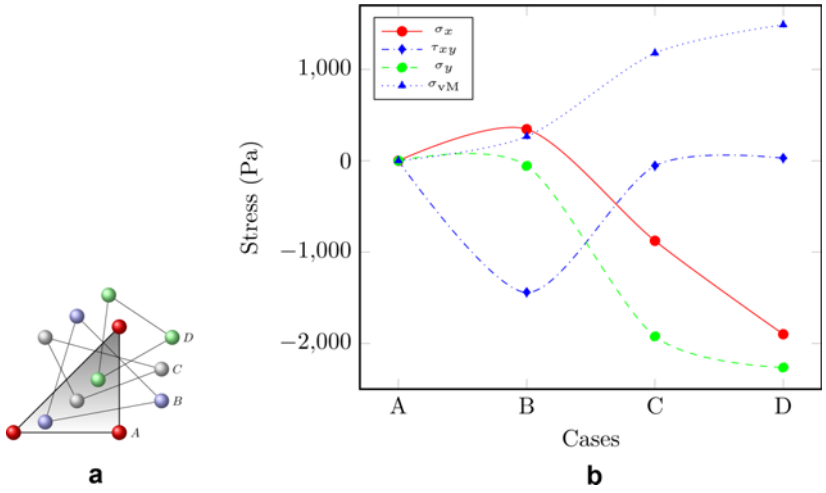

Fig. 8. The simulation results of the complex motion described in Table 2: (a) Schematic of a series of fictitious motions of the triangular element marked on the surface of a specimen. The motion is divided into four different configurations *A*, *B*, C and *D*. Each configuration becomes the current configuration at that time, (b) Calculated stresses σ_x, τ_{xy}, σ_y and σ_{vM} (von Mises stress) with the cell element method subjected to the complex motion described in Table 2 for cases *A*, *B*, *C* and *D*.

hard materials installed on it because of extremely low stiffness. A semi-empirical method, which are validated in a full usage of both finite element methods and mathematical models based on phenomenological approach, is introduced to evaluate the stress-strain responses of biological tissues subjected mechanical loadings. In summary, the present method consists of a series of experimental and numerical procedures, in which there is a development of specimens, construction of cell elements, image processing and deformation assessment. The method could be expanded to more complex arrangements such as three-dimensional motion analysis of head tissues, liver tissues, or blood vessels, where conventional experimental methods fail to function right.

CONFLICT OF INTEREST STATEMENTS

Choi D-K declares that he has no conflict of interest in relation to the work in this article.

REFERENCES

[1] Fung YC. Biomechanics: mechanical properties of living tissues. 2nd ed. New York: Springer; 1993.
[2] Holzapfel GA. Nonlinear solid mechanics: a continuum approach for engineering. New York: John Wiley & Sons; 2000.
[3] Nah C, Lee GB, Lim JY, Kim YH, SenGupta R, Gent AN. Problems in determining the elastic strain energy function for rubber. Int J Non-Linear Mech. 2010; 45(3):232-5.
[4] Haines DW, Wilson WD. Strain-energy density function for rubberlike materials. J Mech Phys Solids. 1979; 27(4):345-60.
[5] Currie PK. Comparison of incompressible elastic strain energy functions over the attainable region of invariant space. Math Mech Solids. 2005; 10(5):559-74.
[6] Puglisi G, Saccomandi G. Multi-scale modelling of rubber-like materials and soft tissues: an appraisal. Proc Math Phys Eng Sci. 2016; 472(2187):20160060.
[7] Steinmann P, Hossain M, Possart G. Hyperelastic models for rubber-like materials: consistent tangent operators and suitability for treloars data. Arch Appl Mech. 2012; 82(9):1183-217.
[8] Horgan CO, Saccomandi G. Constitutive models for compressible nonlinearly elastic materials with limiting chain extensibility. J Elastic. 2004; 77(2):123-38.
[9] Swanson SR, Christensen LW, Ensign M. Large deformation finite element calculations for slightly compressible hyperelastic materials. Comput Struct. 1985; 21(1-2):81-8.
[10] Guo Z, Sluys L. Application of a new constitutive model for the description of rubber-like materials under monotonic loading. Int J Solids Struct. 2006; 43(9):2799-819.
[11] Zhil GP, Gavin HP. United constitutive modeling of rubber-like materials under diverse loading conditions. Int J Eng Sci. 2013; 62(1):90-105.
[12] Merckel Y, Diani J, Brieu M, Caillard J. Constitutive modeling of the anisotropic behavior of mullins softened filled rubbers. Mech Mater. 2013; 57(1):30-41.
[13] Kaliske M, Rothert H. On the nite element implementation of rubber-like materials at finite strains. Eng Comput. 1997; 14(2):216-32.
[14] Sussman T, Bathe KJ. A finite element formulation for nonlinear incompressible elastic and inelastic analysis. Comput Struct. 1987; 26(1-2):357-409.
[15] Miehe C. Aspects of the formulation and finite element implementation of large strain isotropic elasticity. Int J Numer Methods Eng. 1994; 37(12):1981-2004.
[16] Weiss JA, Maker BN, Govindjee S. Finite element implementation of incompressible, transversely isotropic hyperelasticity. Comput Methods Appl Mech Eng. 1996; 135(1-2):107-28.
[17] Sun W, Chaikof EL, Levenston ME. Numerical approximation of tangent moduli for finite element implementations of nonlinear hyperelastic material models. J Biomech Eng. 2008; 130(6):061003.
[18] Germain S, Scherer M, Steinmann P. On inverse form finding for anisotropic materials. Proc Appl Math Mech. 2010; 10(1):159-60.
[19] Govindjee S, Mihalic PA. Computational methods for inverse deformations in quasi-incompressible finite elasticity. Int J Numer Methods Eng. 1998; 43(5):821-38.
[20] Morales DM, Marklund N, Lebold D, Thompson HJ, Pitkanen A, Maxwell WL, Longhi L, Laurer H, Maegele M, Neugebauer E, Graham DI, Stocchetti N, McIntosh TK. Experimental models of traumatic brain injury: do we really need to build a better mousetrap?. Neuroscience. 2005; 136(4):971-89.
[21] Miller K, Chinzei K. Constitutive modelling of brain tissue: experiment and theory. J Biomech. 1997; 30(11-12):1115-21.
[22] Hardy WN, Khalil TB, King AI. Literature review of head injury biomechanics. Int J Impact Eng. 1994; 15(4):561-86.
[23] Ommaya AK, Thibault L, Bandak FA. Mechanisms of impact head injury. Int J Impact Eng. 1994; 15(4):535-60.
[24] Post A, Hoshizaki B, Gilchrist MD. Finite element analysis of the effect of loading curve shape on brain injury predictors. J Biomech. 2012; 45(4):679-83.
[25] Maas A, Stocchetti N, Bullock R. Moderate and severe traumatic brain injury in adults. Lancet Neurol. 2008; 7(8):728-41.
[26] Shafieian M, Darvish KK, Stone JR. Changes to the viscoelastic properties of brain tissue after traumatic axonal injury. J Biomech. 2009; 42(13):2136-42.
[27] Chatelin S, Deck C, Renard F, Kremer S, Heinrich C, Armspach JP, Willinger R. Computation of axonal elongation in head trauma finite element simulation. J Mech Behav Biomed Mater. 2011; 4(8):1905-19.
[28] Case ME. Abusive head injuries in infants and young children. Legal Med. 2007; 9(2):83-7.
[29] Roth S, Vappou J, Raul JS, Willinger R. Child head injury criteria investigation through numerical simulation of real world trauma. Comput Methods Programs Biomed. 2009; 93(1):32-45.
[30] Pan Y, Sullivan D, Shreiber DI, Pelegri AA. Finite element modeling of cns white matter kinematics: use of a 3d rve to determine material properties. Front Bioeng Biotech. 2013; 1(1):19.
[31] Metz H, McElhaney J, Ommaya AK. A comparison of the elasticity of live, dead, and fixed brain tissue. J Biomech. 1970; 3(4):453-8.
[32] Miller K, Chinzei K, Orssengo G, Bednarz P. Mechanical properties of brain tissue in-vivo: experiment and computer simulation. J Biomech. 2000; 33(11):1369-76.
[33] Gefen A, Margulies SS. Are in vivo and in situ brain tissues mechanically simliar?. J Biomech. 2004; 37(9):1339-52.
[34] Feng Y, Okamoto RJ, Namani R, Genin GM, Bayly PV. Measurements of mechanical anisotropy in brain tissue and implications for transversely isotropic material models of white

matter. J Mech Behav Biomed Mater. 2013; 23(1):117-32.
[35] Goriely A, Geers MG, Holzapfel GA, Jayamohan J, Jerusalem A, Sivaloganathan S, Squier W, van Dommelen JA, Waters S, Kuhl E. Mechanics of the brain: perspectives, challenges, and opportunities. Biomech Model Mechanobiol. 2015; 14(5):931-65.
[36] Rashid B, Destrade M, Gilchrist MD. Mechanical characterization of brain tissue in tension at dynamic strain rates. J Mech Behav Biomed Mater. 2014; 33(1):43-54.
[37] Fallenstein GT, Hulce VD, Melvin JW. Dynamic mechanical properties of human brain tissue. J Biomech. 1969; 2(3):217-26.
[38] Pervin F, Chen WW. Dynamic mechanical response of bovine gray matter and white matter brain tissues under compression. J Biomech. 2009; 42(6):731-5.
[39] Holbourn AHS. Mechanics of head injuries. Lancet. 1943; 242(6267):438-41.
[40] Margulies SS, Thibault LE, Gennarelli TA. Physical model simulations of brain injury in the primate. J Biomech. 1990; 23(8):823-36.
[41] Sabet AA, Christoforou E, Zatlin B, Genin GM, Bayly PV. Deformation of the human brain induced by mild angular head acceleration. J Biomech. 2008; 41(2):307-15.
[42] Ljung C. A model for brain deformation due to rotation of the skull. J Biomech. 1975; 8(5):263-74.
[43] Bycroft GN. Mathematical model of a head subjected to an angular acceleration. J Biomech. 1973; 6(5):487-95.
[44] Misra JC, Chakravarty S. A study on rotational brain injury. J Biomech. 1984; 17(7):459-66.
[45] Hickling R, Wenner ML. Mathematical model of a head subjected to an axisymmetric impact. J Biomech. 1973; 6(2):115-32.
[46] Firoozbakhsh KK, DeSilva CN. A model of brain shear under impulsive torsional loads. J Biomech. 1975; 8(1):65-73.
[47] Miller K, Chinzei K. Mechanical properties of brain tissue in tension. J Biomech. 2002; 35(4):483-90.
[48] Sayed TE, Mota A, Fraternali F, Ortiz M. Biomechanics of traumatic brain injury. Comput Methods Appl Mech Eng. 2008; 197:4692-701.
[49] Prevost TP, Balakrishnan A, Suresh S, Socrate S. Biomechanics of brain tissue. Acta Biomater. 2011; 7(1):83-95.
[50] Brands DW, Peters GW, Bovendeerd PH. Design and numerical implementation of a 3-d non-linear viscoelastic constitutive model for brain tissue during impact. J Biomech. 2004; 37(1):127-34.
[51] Mihai LA, Chin L, Janmey PA, Goriely A. A comparison of hyperelastic constitutive models applicable to brain and fat tissues. J Royal Soc Interface. 2015; 12(110):20150486.
[52] Soza G, Grosso R, Nimsky C, Hastreiter P, Fahlbusch R, Greiner G. Determination of the elasticity parameters of brain tissue with combined simulation and registration. Int J Med Robot. 2005; 1(3):87-95.
[53] Libertiaux V, Pascon F, Cescotto S. Experimental vitrification of brain tissue incompressibility using digital image correlation. J Mech Behav Biomed Mater. 2011; 4(7):1177-85.
[54] Hagemann A, Rohr K, Stiehl H. Coupling of fluid and elastic models for biomechanical simulations of brain deformations using FEM. Med Image Anal. 2002; 6(4):375-88.
[55] OGara PT. Aortic aneurysm. Circulation. 2003; 107(6):e43-5.
[56] Fung YC, Fronek K, Patitucci P. Pseudoelasticity of arteries and the choice of its mathematical expression. Am J Physiol. 1979; 237(5):H620-31.
[57] Horgan C, Saccomandi G. A description of arterial wall mechanics using limiting chain extensibility constitutive models. Biomech Model Mechanobiol. 2003; 1(4):251-66.
[58] Holzapfel GA, Weizscker HW. Biomechanical behavior of the arterial wall and its numerical characterization. Comput Biol Med. 1998; 28(4):377-92.
[59] Hayashi K. Experimental approaches on measuring the mechanical properties and constitutive laws of arterial walls. J Biomech Eng. 1993; 115(4B):481-8.
[60] Carew TE, Vaishnav RN, Patel DJ. Compressibility of the arterial wall. Circ Res. 1968; 23(1):61-8.
[61] Nolan DR, McGarry JP. On the compressibility of arterial tissue. Ann Biomed Eng. 2016; 44(4):993-1007.
[62] Chuong CJ, Fung YC. Compressibility and constitutive equation of arterial wall in radial compression experiments. J Biomech. 1984; 17(1):35-40.
[63] Lally C, Reid AJ, Prendergast PJ. Elastic behavior of porcine coronary artery tissue under uniaxial and equibiaxial tension. Ann Biomed Eng. 2004; 32(10):1355-64.
[64] Gasser TC, Ogden RW, Holzapfel GA. Hyperelastic modelling of arterial layers with distributed collagen fibre orientations. J Royal Soc Interface. 2006; 3(6):15-35.
[65] Helderman F, Manoch IJ, Breeuwer M, Kose U, Schouten O, van Sambeek MR, Poldermans D, Pattynama PT, Wisselink W, van der Steen AF, Krams R. A numerical model to predict abdominal aortic aneurysm expansion based on local wall stress and stiffness. Med Biol Eng Comput. 2008; 46(11):1121-7.
[66] Di Martino ES, Vorp DA. Effect of variation in intraluminal thrombus constitutive properties on abdominal aortic aneurysm wall stress. Ann Biomed Eng. 2003; 31(7):804-9.
[67] Rodriguez JP, Martufi G, Doblare M, Finol EA. The effect of material model formulation in the stress analysis of abdominal aortic aneurysms. Ann Biomed Eng. 2009; 37(11):2218-21.
[68] Raghavan ML, Webster MW, Vorp DA. Ex vivo biomechanical behavior of abdominal aortic aneurysm: assessment using a new mathematical model. Ann Biomed Eng. 1996; 24(5):573-82.
[69] Tong J, Holzapfel GA. Structure, mechanics, and histology of intraluminal thrombi in abdominal aortic aneurysms. Ann Biomed Eng. 2015; 43(7):1488-501.
[70] Simon BR, Kaufmann MV, McAfee MA, Baldwin AL. Finite element models for arterial wall mechanics. J Biomech Eng. 1993; 115(4B):489-96.
[71] Doyle BJ, Callanan A, McGloughlin TM. A comparison of modelling techniques for computing wall stress in abdominal aortic aneurysms. Biomed Eng Online. 2007; 6(1):38.
[72] Chuong CJ, Fung YC. Three-dimensional stress distribution in arteries. J Biomech Eng. 1983; 105(3):268-74.
[73] Balzani D, Brinkhues S, Holzapfel GA. Constitutive framework for the modeling of damage in collagenous soft tissues with application to arterial walls. Comput Methods Appl Mech Eng. 2012; 213-6:139-51.
[74] Volokh KY. Modeling failure of soft anisotropic materials with application to arteries. J Mech Behav Biomed Mater. 2011; 4(8):1582-94.
[75] Molony DS, Callanan A, Kavanagh EG, Walsh MT, McGloughlin TM. Fluid-structure interaction of a patient-specific abdominal aortic aneurysm treated with an endovascular stent-graft. Biomed Eng Online. 2009; 8(1):24.
[76] Xenos M, Rambhia SH, Alemu Y, Einav S, Labropoulos N, Tassiopoulos A, Ricotta JJ, Bluestein D. Patient-based abdominal aortic aneurysm rupture risk prediction with fluid structure interaction modeling. Ann Biomed Eng. 2010; 38(11):3323-37.
[77] Scotti CM, Shkolnik AD, Muluk SC, Finol EA. Fluid-structure interaction in abdominal aortic aneurysms: effects of asymmetry and wall thickness. Biomed Eng Online. 2005; 4(1):64.
[78] Dorfmann A, Wilson C, Edgar ES, Peattie RA. Evaluating patient-specific abdominal aortic aneurysm wall stress based on flow-induced loading. Biomech Model Mechanobiol. 2010; 9(2):127-39.
[79] Liu Y, Dang C, Garcia M, Gregersen H, Kassab GS.

Surrounding tissues affect the passive mechanics of the vessel wall: theory and experiment. Am J Physiol Heart Circ Physiol. 2007; 293(6):H3290-300.
[80] Sever A, Rheinboldt M. Unstable abdominal aortic aneurysms: a review of mdct imaging features. Emerg Radiol. 2016; 23(2):187-96.
[81] Taylor CA, Steinman DA. Image-based modeling of blood flow and vessel wall dynamics: applications, methods and future directions. Ann Biomed Eng. 2010; 38(3):1188-203.
[82] Maier A, Gee MW, Reeps C, Eckstein HH, Wall WA. Impact of calcification on patient-specific wall stress analysis of abdominal aortic aneurysms. Biomech Model Mechanobiol. 2010; 9(5):511-21.
[83] Bader H. Dependence of wall stress in the human thoracic aorta on age and pressure. Circ Res. 1967; 20(3):354-61.
[84] Weizsacker HW, Holzapfel GA, Desch GW, Pascale K. Strain energy density function for arteries from different topographical sites. Biomedizinische Technik. 1995; 40(s2):139-41.
[85] Davis FM, Luo Y, Avril S, Duprey A, Lu J. Local mechanical properties of human ascending thoracic aneurysms. J Mech Behav Biomed Mater. 2016; 61(1):235-49.
[86] Shum J, Xu A, Chatnuntawech I, Finol EA. A framework for the automatic generation of surface topologies for abdominal aortic aneurysm models. Ann Biomed Eng. 2011; 39(1):249-59.
[87] Dal H, Goktepe S,, Kaliske M, Kuhl E. A fully implicit finite element method for bidomain models of cardiac electromechanics. Comput Methods Appl Mech Eng. 2013; 253(1):323-36.
[88] Rossi S, Ruiz-Baier R, Pavarino LF, Quarteroni A. Orthotropic active strain models for the numerical simulation of cardiac biomechanics. Int J Numer Methods Biomed Eng. 2012; 28(6-7):761-88.
[89] Wagner DR, Lotz JC. Theoretical model and experimental results for the nonlinear elastic behavior of human annulus fibrous. J Orthop Res. 2004; 22(4):901-9.
[90] Odegard GM, Donajue TL, Morrow DA, Kaufman KR. Constitutive modeling of skeletal muscle tissue with an explicit strain-energy function. J Biomech Eng. 2008; 130(6):061017.
[91] Grujicic M, Pandurangan B, Arakere G, Bell WC, He T, Xie X. Seat-cushion and soft-tissue material modeling and a finite element investigation of the seating comfort for passenger-vehicle occupants. Mater Design. 2009; 30(10):4273-85.
[92] Maquet PG, Pelzer GA. Evolution of the maximum stress in osteo-arthritis of the knee. J Biomech. 1977; 10(2):107-17.
[93] Holzapfel GA, Eberlein R, Wriggers P, Weizsacker HW. Large strain analysis of soft biological membranes: formulation and finite element analysis. Comput Methods Appl Mech Eng. 1996; 132(1-2):45-61.
[94] Lu J, Zhou X, Raghavan ML. Inverse elastostatic stress analysis in pre-deformed biological structures: demonstration using abdominal aortic aneurysms. J Biomech. 2007; 40(3):693-6.
[95] Kroon M, Holzapfel GA. Estimation of the distributions of anisotropic, elastic properties and wall stresses of saccular cerebral aneurysms by inverse analysis. Proc Math Phys Eng Sci. 2008; 464(2092):807-25.
[96] Krishnamurthy G, Ennis DB, Itoh A, Bothe W, Swanson JC, Karlsson M, Kuhl E, Miller DC, Ingels NB. Material properties of the ovine mitral valve anterior leaflet in vivo from inverse finite element analysis. Am J Physiol Heart Circ Physiol. 2008; 295(3):H1141-9.
[97] Samani A, Bishop J, Luginbuhl C, Plewes DB. Measuring the elastic modulus of ex vivo small tissue samples. Phys Med Biol. 2003; 48(14):2183-98.
[98] Chen EJ, Novakofski J, Jenkins WK, OBrien WD. Young's modulus measurements of soft tissues with application to elasticity imaging. IEEE Trans Ultrason Ferr. 1996; 43(1):191-4.
[99] Chenevert TL, Skovoroda AR, ODonnell M, Emelianov SY. Elasticity reconstructive imaging by means of stimulated echo mri. Magn Reson Med. 1998; 39(3):482-90.
[100] Erkamp RQ, Wiggins P, Skovoroda AR, Emelianov SY, ODonnell M. Measuring the elastic modulus of small tissue samples. 1998; 20(1):17-28.
[101] Krouskop TA, Wheeler TM, Kallel F, Garra BS, Hall T. Elastic moduli of breast and prostate tissues under compression. Ultrason Imaging. 1998; 20(4):260-74.
[102] Samani A, Bishop J, Yaffe MJ, Plewes DB. Biomechanical 3-d finite element modeling of the human breast using mri data. IEEE Trans Med Imaging. 2001; 20(4):271-9.
[103] Misra S, Ramesh KT, Okamura AM. Modelling of non-linear elastic tissues for surgical simulation. Comput Methods Biomech Biomed Eng. 2010; 13(6):811-8.
[104] Miller K, Joldes G, Lance D, Wittek A. Total lagrangian explicit dynamics finite element algorithm for computing soft tissue deformation. Int J Numer Methods Biomed Eng. 2007; 23(2):121-134.
[105] Portnoy S, Yarnitzky G, Yizhar Z, Kristal A, Oppenheim U, Siev-Ner I, Gefen A. Real-time patient-specific nite element analysis of internal stresses in the soft tissues of a residual limb: a new tool for prosthetic fitting. Ann Biomed Eng. 2007; 35(1):120-35.
[106] Niroomandi S, Alfaro I, Cueto E, Chinesta F. Real-time deformable models of non-linear tissues by model reduction techniques. Comput Methods Programs Biomed. 2008; 91(3):223-31.
[107] Baillargeon B, Rebelo N, Fox DD, Taylor RL, Kuhl E. The living heart project: a robust and integrative simulator for human heart function. Eur J Mech A-Solid. 2014; 48(1):38-47.
[108] Miller K. Constitutive model of brain tissue suitable for finite element analysis of surgical procedures. J Biomech. 1999; 32(5):531-7.
[109] Bahn Y, Choi DK. Numerical and experimental study on mechanical properties of gelatin as substitute for brain tissue. Trans Kor Soc Mech Eng B. 2015; 39(2):169-76.
[110] Bonet J, Wood RD. Nonlinear continuum mechanics for finite element analysis. Cambridge: Cambridge University Press; 1997.